Longitudinal, transversal and averaged mechanical stresses that the bridge suffers when maximum acceleration is applied are shown in fig. 4.40. In this case, lower stresses are applied to the bridges due to their low stiffness. It can also be observed that in this case, longitudinal and transversal stress values approximately have the same magnitude. That is, in an L-shaped bridge, due to its geometry, mechanical stresses are approximately equally distributed both in the transversal and longitudinal directions.

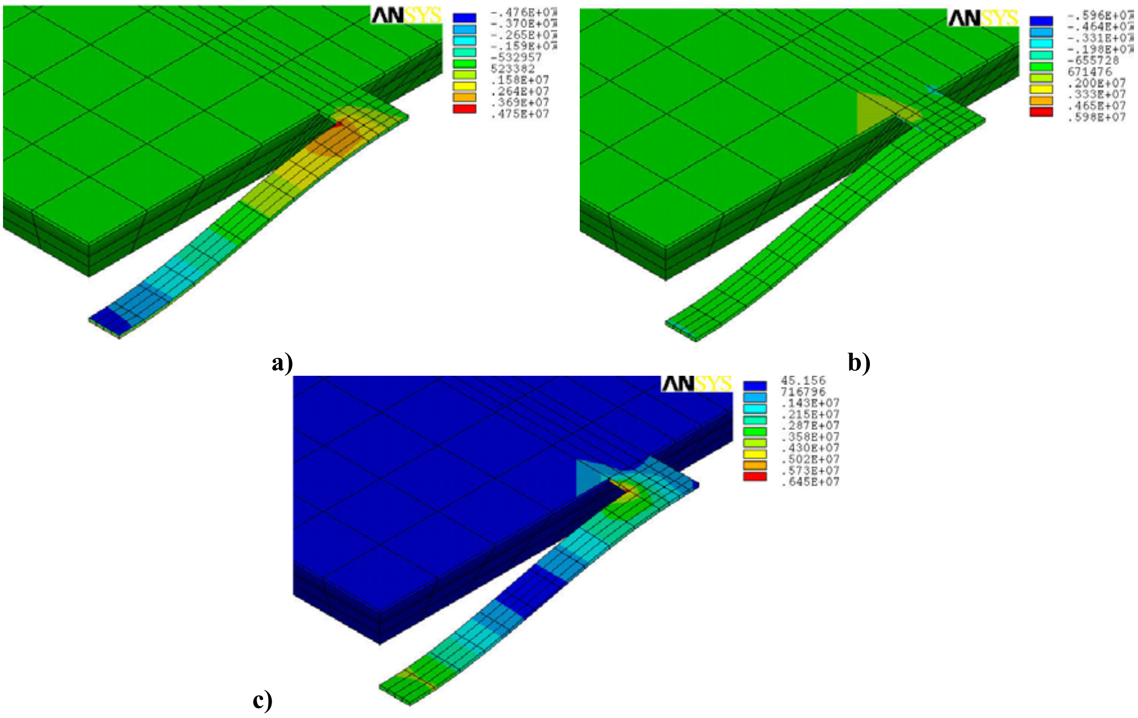

Fig 4.40. a) Lateral and b) transversal stress distribution on the bridges of the misalignment accelerometer. c) Average stress value considering 3D movement.

Finally, modal simulations were done so as to fix the structure vibrational modes. The first vibration mode has a natural frequency of 488.75Hz. The deformation of the structure for this mode is shown in fig. 4.38d. Its significant reduction, as compared to the diaphragm accelerometer, is logical due to the different acceleration ranges for which they were designed. This device has been designed for ±1g range and so its stiffness is lower as compared to the previously presented diaphragm accelerometer design.

Acceleration	Y_{max} (nm/g)	S_l (MPa)	S_t (MPa)
In z axis	1.050	4.7	4.6
In y axis	0.105*		
In x axis	0.202		

* For misalignment accelerometers with centered waveguides, there exists no movement.

Table 4.10: a) Maximum displacement in the *y*-axis (Y_{max}) for accelerations in the three directions and longitudinal and transversal mechanical stresses.

Opto-mechanical specifications of the misalignment accelerometer are summarized in table 4.11. It has been seen that although the configuration proposed is not able to distinguish the acceleration sign at which it is submitted, the fact that it is self-aligned and that has extremely high failure losses are clear advantages as compared to the diaphragm optical accelerometer. Mechanical properties have been adapted so as to fulfill the optical requirements. In this case, however, L-shaped bridges have been used, showing a lower and more uniform stress distribution for approximately the same range as compared to straight bridges. Moreover, they provide with a higher sensitivity for the same chip area. Straight bridges would mean an excessively large device that would harden its manipulation and would increase its cost. Normal frequencies obtained by simulations are much lower as compared to these from the diaphragm accelerometer. This is mainly due to the fact that for detecting low acceleration variations large bridges or low stiff structures are needed, with the consequently decrease of the natural frequency.

Optical considerations

Waveguide width			Distance between waveguides (µm)		Failure losses in z axis (dB)	Failure losses in x axis (dB)
Input (µm)	Sensing (µm)	Output (µm)	With mass	Without mass		
14	30	50	24	4044	18.1	1.3

Mechanical considerations

Bridge Length (µm)	Top mass area (μm^2)	Sensitivity (dB/µm)	Frequency (Hz)	Span (µm)	Maximum displacement		
					x (µm/g)	z (µm/g)	y (µm/g)
1347	4015x4015	4.5	489	1	0.202	0	1.050

Table 4.11. Basic specifications for the misalignment -based optical accelerometer.

This chapter has been focused on analyzing the viability and goodness of the modifications proposed for several existing integrated optical devices, ranging from simple waveguides to optical accelerometers. Once the simulations have been done, and using the previously described technological steps, they will be obtained. Results and comparison between simulation and experimental will be presented in the following chapter.

Bibliography

[1] I.Garcés. *Estudio Teórico y Desarrollo Experimental de Guías de Onda Ópticas en Tecnología de Silicio: Aplicación al Diseño de Sensores Optoquímicos*, Thesis. 1996. Universidad de Zargoza. Departamento de Física Aplicada.

[2] M.Kuznetsov. *Cascaded Coupler Mach-Zehnder Channel Dropping Filters for Wavelength-Division Multiplexed Optical Systems*. J.Light.Tech. 12[2], 226-230. 1994.

[3] J.Subías, R.Alonso, F.Villuendas, J.Pelayo. *Wavelength Selective Optical Fiber Couplers Based on Longitudinal Fabry-Perot Structures.* J.Light.Tech. 12[7], 1129-1135. 1994.

[4] B.E.Little. *Optical-Induced Spectral Tuning in Grating-Assisted Nonlinear Couplers*. J.Light.Tech. 12[5], 774-783. 1994.

[5] K.Benaissa, A.Nathan, S.T.Chu, W.P.Huang. *Simulation and Fabrication of ARROW Directional Couplers.* SPIE 2641, 49-54. 1995.

[6] A.Chowdhury, L.McCaughan. *Continuously Phase-Matched M-Waveguides for Second-Order Nonlinear Upconversion*. IEEE Phot.Tech.Lett. 12[5], 486-488. 2000.

[7] A.Llobera, I.Salinas, I.Garcés, A.Merlos, C.Domínguez. *Effect of the Wall Tilt on the Optical Properties of Integrated Directional Couplers*. Opt.Lett. 25[8], 601-603. 2002.

[8] J.Gehler, A.Bräuer, W.Karthe. *Remote Coupling over 93µm Using ARROW Waveguides in Strip Configuration*. Electr.Lett. 30[3], 218-220. 1994.

[9] M.Mann, U.Trutschel, C.Wächter, L.Leine, F.Lederer. *Directional Coupler Based on an Antiresonant Relfecting Optical Waveguide*. Opt.Lett. 16[11], 805-807. 1991.

[10] B.J.Luff, J.S.Wilkinson, J.Pichler, U.Hollenbach, J.Ingenhoff, N.Fabricius. *Integrated Optical Mach-Zehnder Biosensor*. J.Light.Tech. 16[4], 583-592. 1998.

[11] H.Sasaki, I.Anderson. *Theoretical and Experimental Studies on Active Y-Junctions in Optical Waveguides*. IEEE J.Quant.Elect. QE-14[11], 883-892. 1978.

[12] R.Baets, P.A.Lagasse. *Calculation of Radiation Loss in Integrated-optic Tapers and Y-Junctions*.

Appl.Optics. 21[11], 1972-1978. 1982.

[13] J.van der Tol, J.W.Pedersen, E.Metaal, Y.S.Oei, F.H.Groen, P.Demeester. *Sharp Vertices in Asymmetric Y-Junctions by Double Masking.* IEEE Phot.Tech.Lett. 6[2], 249-251. 1994.

[14] C.Wei, F.H.Groen, M.K.Smit, I.Moerman, P.van Daele, R.Baets. *Integrated Optical Elliptic Couplers: Modeling, Design and Applications*. J.Light.Tech. 15[5], 906-912. 1997.

[15] K.Okamoto, A.Sugita. *Flat Spectral Response Arrayed-Waveguide Grating With Parabolic Waveguide Horns.* Electr.Lett. 32[18], 1661-1662. 1996.

[16] F.Prieto, L.M.Lechuga, A.Calle, A.Llobera, C.Domínguez. *Optimized Silicon Antiresonant Reflecting Optical Waveguides for Sensing Applications*. J.Light.Tech. 19[1], 75-83. 1-1-2001.

[17] R.G.Heideman, P.V.Lambeck. *Remote Opto-Chemical Sensing with Extreme Sensitivity: Design, Fabrication and Performance of a Pigtailed Integrated Optical Phase-Modulated Mach-Zehnder Interferometer System.* Sens.& Act.B B-61, 100-127. 1999.

[18] G.H.Jin, Y.K.Zou, V.Fuflyigin, S.W.Liu, Y.L.Lu, J.Zhao *et al. PLZT Film Waveguide Mach-Zehnder Electrooptic Modulator*. J.Light.Tech. 18[6], 807-811. 2000.

[19] R.A.Soref, D.L.McDaniel, B.R.Bennet. *Guided-Wave Intensity Modulators Using Amplitude-and-Phase Perturbations.* J.Light.Tech. 6[3], 437-444. 1988.

[20] L.B.Soldano, E.C.Pennings. *Optical Multi-Mode Interference Devices Based on Self-Imaging: Principles and Applications*. J.Light.Tech. 13[4], 615-627. 1995.

[21] W.Lucosz, C.Stamm. *Integrated Optical Interferometer as Relative Humidity Sensor and Differential Refractometer*. Sens.& Act.A 25[27], 185-188. 1991.

[22] *F.Prieto. Sensores Interferométricos Mach-Zehnder Integrados Basados en Guías de Onda ARROW para Aplicaciones Biosensoras*, Thesis. 2002. Universidad Autónoma de Madrid.

[23] F.Prieto, A.Llobera, D.Jiménez, C.Domínguez, A.Calle, L.M.Lechuga. *Design and Analysis of Silicon Antiresonant Reflecting Optical Waveguides for Evanescent Field Sensor.* J.Light.Tech. 18[7], 966-972. 2000.

[24] K.A.Remley, A.Weisshaar. *Design and Analysis of a Silicon-Based Antiresonant reflecting Optical Waveguide Chemical Sensor*. Opt.Lett. 21[16], 1241-1243. 1996.

[25] K.E.Burcham, G.N.de Brabander, J.T.Boyd. *Micromachined Silicon Cantilever Beam Accelerometer Incorporating an Integrated Optical Waveguide.* SPIE 1793 Integrated Optics and Microstructures, 12-18. 1992.

[26] J.A.Plaza. *µAcelerómetros de Silicio*, Thesis. 1997. Universitat Autònoma de Barcelona.